

Journal Pre-proofs

Synthesis of New Hetero-Arylidene-9(10*H*)-Anthrone Derivatives and Their Biological Evaluation

Catarina Roma-Rodrigues, Gabriela Malta, Daniela Peixoto, Luísa M. Ferreira, Pedro V. Baptista, Alexandra R. Fernandes, Paula S. Branco

PII: S0045-2068(19)32209-6
DOI: <https://doi.org/10.1016/j.bioorg.2020.103849>
Reference: YBIOO 103849

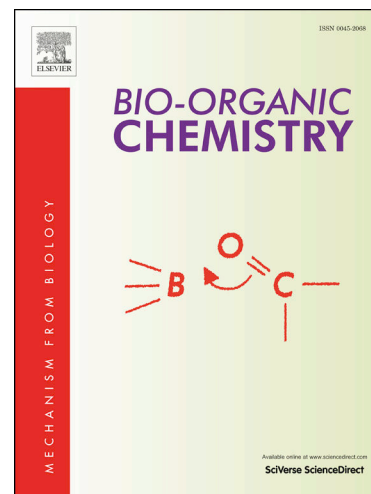
To appear in: *Bioorganic Chemistry*

Received Date: 26 December 2019
Revised Date: 9 April 2020
Accepted Date: 10 April 2020

Please cite this article as: C. Roma-Rodrigues, G. Malta, D. Peixoto, L.M. Ferreira, P.V. Baptista, A.R. Fernandes, P.S. Branco, Synthesis of New Hetero-Arylidene-9(10*H*)-Anthrone Derivatives and Their Biological Evaluation, *Bioorganic Chemistry* (2020), doi: <https://doi.org/10.1016/j.bioorg.2020.103849>

This is a PDF file of an article that has undergone enhancements after acceptance, such as the addition of a cover page and metadata, and formatting for readability, but it is not yet the definitive version of record. This version will undergo additional copyediting, typesetting and review before it is published in its final form, but we are providing this version to give early visibility of the article. Please note that, during the production process, errors may be discovered which could affect the content, and all legal disclaimers that apply to the journal pertain.

© 2020 Published by Elsevier Inc.



Synthesis of New Hetero-Arylidene-9(10*H*)- Anthrone Derivatives and Their Biological Evaluation

Catarina Roma-Rodrigues,^[b] Gabriela Malta,^[a] Daniela Peixoto,^[a] Luísa M. Ferreira,^[a] Pedro V. Baptista,^[b] Alexandra R. Fernandes,^{[b]} and Paula S. Branco^{*[a]}*

^aLAQV-REQUIMTE, DQ, NOVA School of Science and Technology, 2829-516, Caparica, Portugal.

^bUCIBIO, DCV, NOVA School of Science and Technology, 2829-516, Caparica, Portugal.

To whom correspondence should be addressed: Paula S. Branco, Chemistry Department, LAQV-REQUIMTE, Faculdade de Ciências e Tecnologia, Universidade Nova de Lisboa, 2829-516 Caparica, Portugal. Tel: +351 21 2948300; e-mail: paula.branco@fct.unl.pt; Alexandra R. Fernandes UCIBIO, DCV, Faculdade de Ciências e Tecnologia, Universidade Nova de Lisboa, 2829-516 Caparica, Portugal. Tel: +351 21 2948300; e-mail: ma.fernandes@fct.unl.pt.

ABSTRACT

New hetero-arylidene-9(10*H*)-anthrone derivatives (**1**) were synthesized from reaction of 1,2-dimethyl-3-alkyl imidazolium salts (**2**) and 9-anthracenecarboxaldehyde. Ion exchange of the anion with dioctyl sulfosuccinate and lithium bis(trifluoromethanesulfonyl)imide led to the preparation of other derivatives. The antiproliferative effect of the compounds was evaluated in human ovarian (A2780) and colorectal (HCT116) carcinoma cell lines and in normal primary human fibroblasts. Compound **1** presented an antiproliferative effect related to the imidazolium pattern of substitution with compounds having a decyl group at the R-position (**1c** and **3c**) showing the highest cytotoxic activities in all cell lines independently of the counter ion. Compounds **1b** and **1c** internalize A2780 cancer cells via a passive or an active transport, respectively, inducing A2780 cell death via an extrinsic apoptosis (**1b**) or intrinsic apoptosis and oncosis (**1c**). The localization of both compounds in the cytoplasm coupled to the absence of reactive oxygen species (ROS) induction suggest that the mechanisms of toxicity might be different than those of other anthracyclines currently used in chemotherapy.

KEYWORDS. : Arylidene-anthrone derivatives • imidazolium chemistry • ovarian cancer • proliferation inhibition • cell apoptosis.

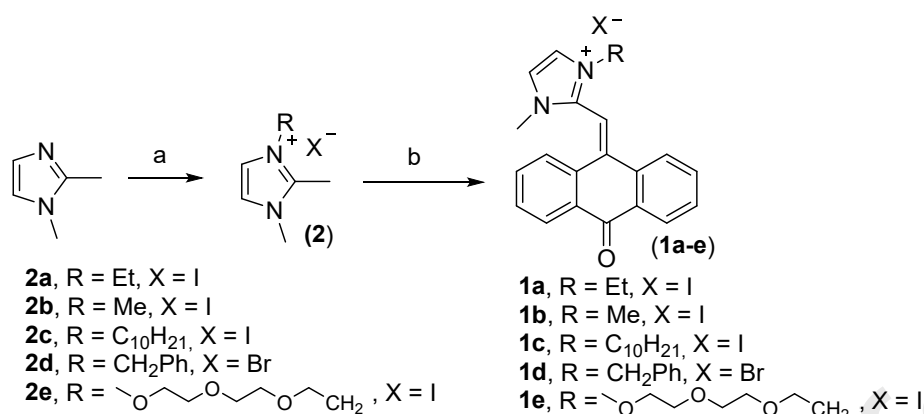
1. Introduction

Anthraquinones are privileged structures from natural sources, such as pigments, vitamins, and enzymes. Besides their utilization as dyes, anthraquinone derivatives have long been used in medical applications, [1, 2] with several anthraquinone derivatives showing interesting medicinal uses, such as anticancer, antibacterial, anti-inflammatory, antioxidant, antidiabetic and antiviral [2-4]. The anticancer action of anthraquinone derivatives has been associated to DNA intercalation due to the flat aromatic anthraquinone core [5]. Some examples include doxorubicin,[3] daunorubicin and carminomycin [4]. Despite the widespread use of these compounds in the clinics, there is a high correlation between anthracycline based chemotherapy and cardiotoxicity, [6] which has prompted for the search of novel drugs with lower side effects. The anthrone analogs, 10-substituted benzylidene anthrones are compounds similar to anthraquinone where a carbonyl group is replaced by a substituted alkene. Some anthrone derivatives have shown potent *in vitro* antitumor activity, [7, 8] with some compounds acting as inhibitors of tubulin polymerization [9, 10]. Syntheses of 10-substituted benzylidene anthrones has been reported by a straightforward aldol-type condensation reaction of anthrone and substituted benzaldehydes under acidic or basic conditions [8, 9] or under microwave irradiation [11]. Recently, we described for the first time a hetero arylidene-9(10*H*)-anthrone (**1a**) formed by reaction of 9-anthracenecarboxaldehyde with 1,2-dimethyl-3-ethylimidazolium iodide (**2a**) under basic conditions (Scheme 1) [12]. The detailed synthetic mechanism was presented demonstrating that, N-heterocyclic olefins (NHO) derived from **2** were postulated as reactive species in the pathway for the formation of **1**. As shown for other anthrones, compound **1a** intercalates with CT-DNA ($K_b = 2.0(\pm 0.20) \times 10^5 \text{ M}^{-1}$), being able to displace GelRed from the DNA double-strand, resulting in the quenching of fluorescence of the GelRed-CT-DNA system (K_{SV}

= $3.3 \pm 0.3 \times 10^3 \text{ M}^{-1}$). [5, 12] Still, compound **1a** showed neither cytotoxicity in ovarian (A2780) and colorectal (HCT116) carcinoma cell lines nor in human healthy fibroblasts [12]. Since this compound is capable to intercalate within the DNA structure but it does not present any cytotoxicity might be related to its inability to cross the cellular membrane. We hypothesized that suitably designed derivatives might surpass this limitation and, herein, we report the preparation and characterization of analogues of **1a** that could show increased antiproliferative effects on tumor cells with low or no effect in normal cells. From the resulting selective library of compounds, the most interesting were further studied concerning their biological effects in ovarian carcinoma cells.

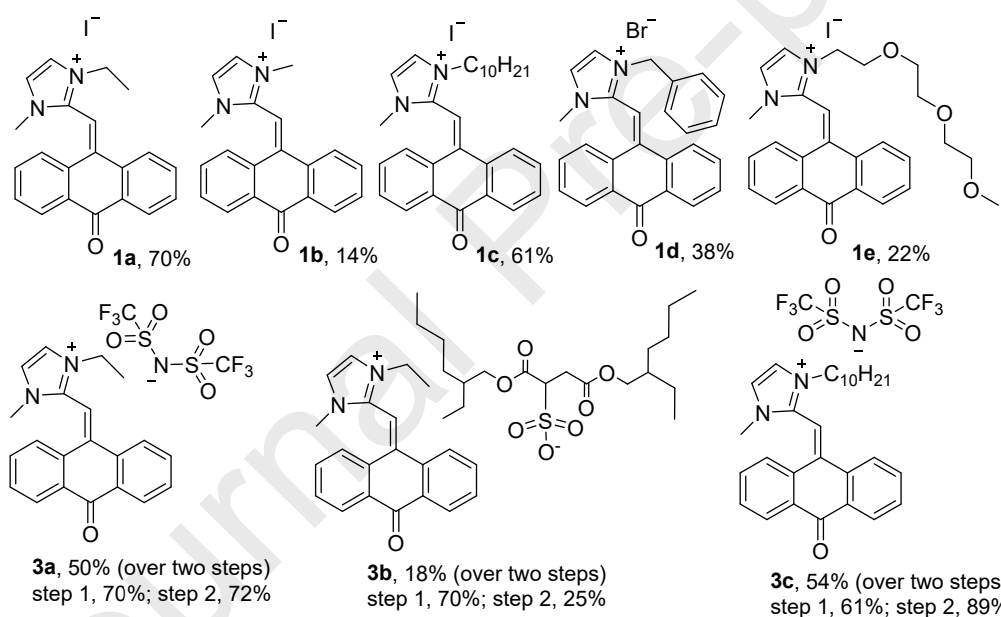
2. Results and Discussion

Synthesis. Two main approaches were followed towards preparation of new hetero arylidene-9(10*H*)-anthrones (**1** and **3**), using the imidazolium ring substituents and the counter anion as targets for structural diversity. For this purpose, several imidazolium salts (**2**) were prepared by alkylation of 1,2-dimethylimidazole using the appropriated alkyl halide in dry THF, under reflux according to a modified literature procedure of Blümel [13]. The imidazolium salts precipitated from the reaction medium and were filtered to provide **2** in good to high yield (65%-95%) (Scheme 1). Spectroscopic data of **2a-d** are in accordance with literature [14, 15]. For the synthesis of **2e**, it was necessary the preparation of the 3-{2-[2-(2-methoxyethoxy)ethoxy]ethyl} iodide from triethylene glycol monomethyl ether following a reported procedure [16]. The imidazolium salts **2a-e** thus prepared were subsequent used for the preparation of **1a-e** following our previously described procedure (Scheme 1) [12]. The yields obtained were very low to high (14 to 70%, Table 1).

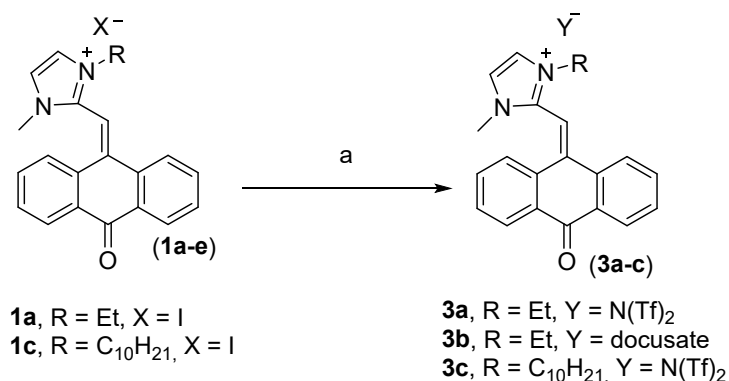


Scheme 1. Synthesis of hetero arylidene-9(10*H*)-anthrone (**1**) derivatives: a) R-X (1 to 1.2 equiv), THF, reflux. b) 9-anthracenecarboxaldehyde, Cs₂CO₃, THF, room temperature, eight days.

Table 1. Scope of substrates of the synthesized hetero arylidene-9(10*H*)-anthrone (**1**).



To proceed for the anion exchange it was followed the procedure of Jordão [17] involving precipitation of the dioctyl sulfosuccinate (docusate) or the bistriflimide (NTf₂) imidazolium salts from an aqueous solution (Scheme 2). The procedure allowed the preparation of hetero arylidene-9(10*H*)-anthrones (**3a-c**) in low to high yield (25% to 89%, Table 1).



Scheme 2. Synthesis of hetero arylidene-9(10*H*)-anthrone (**3**) derivatives: a) **1a** or **1c** (1 equiv), Sodium docusate (1.1 equiv) or Li(N(Tf)₂) (1.1 equiv), H₂O.

These counter anions were selected to correlate the antiproliferative effect with the structural modifications. Docusate is a nontoxic medication used to treat occasional constipation and its effect may not necessarily be entirely due to its surfactant properties, [18] and we expected its long and ramified alkyl chain to penetrate the cellular membrane. Also, the same propriety will be assessed by the substitution pattern at the imidazolium ring. The effect of imidazole ionic liquids (IL) alkyl chains on the cytotoxicity against human lung carcinoma A549 cell line using different classes of cations and anions was evaluated by Chen et al., [19] and showed that compounds with longer non-polar alkyl chains presented higher cytotoxicity when combined with the same anion. As for the anion bistriflimide, it has been widely used in ionic liquids (IL) since it is a less toxic and more stable non-coordinating ion than "traditional" counterions, such as tetrafluoroborate.

Cell viability. To evaluate the importance of the R- substitution and the counter ion in the cytotoxicity of the hetero arylidene-9(10*H*)-anthrone derivatives, the antiproliferative effect of compounds **1b-e** and **3a-c** was assessed by the MTS assay in human ovarian carcinoma cells (A2780), colorectal carcinoma cells (HCT116), and in normal primary human fibroblasts. The MTS assay is based on the formation of a

colored product – formazan, by the reduction of 3-(4,5-dimethylthiazol-2-yl)-5-(3-carboxymethoxyphenyl)-2-(4-sulfophenyl)-2*H*-tetrazolium inner salt (MTS) catalyzed by dehydrogenases enzymes [20]. Hence, the quantity of produced formazan is proportional to the number and metabolic rate of cells in culture. From the MTS data, it was possible to calculate the IC₅₀ for each compound. Regardless of the counter ion, compounds with an ethyl group (**1a**, **3a** and **3b**, Scheme 1 and Scheme 2) showed the lowest antiproliferative activity, with an IC₅₀ higher than 50 μM in HCT116 colorectal carcinoma cells and fibroblasts and higher than 50 μM for **1a**, 22.9 ± 1.7 μM for **3a** and 43.6 ± 0.6 μM for **3b** in A2780 (Table 2, Figure 1, Figure S1-S3) [12]. Compounds **1c** and **3c**, both with a decyl group (C₁₀H₂₁) at the R-substitution location and different counter-ions (Scheme 1), showed the highest antiproliferative effect in A2780 tumor cell line (IC₅₀ of 1.1 ± 0.1 μM for **1c** and 1.3 ± 0.1 μM for **3c**; Table 2, Figure 1) suggesting that the R-substitution on the hetero arylidene-9(10*H*)-anthrone has an important role in the antiproliferative activity of the compounds.

Table 2. IC₅₀ values after 48 h incubation of compounds **1a-e** and **3a-c** in human cancer cell lines A2780 and HCT116 and normal human dermal fibroblasts.

Compound	R-Group	Counter ion X ⁻ or Y ⁻	IC ₅₀ (μM)		
			A2780	HCT116	Fibroblasts
1a [12]	Et	I	> 50	> 50	> 50
1b	Me	I	12.5 ± 0.5	> 50	> 50
1c	C ₁₀ H ₂₁	I	1.1 ± 0.1	5.0 ± 0.7	8.1 ± 1.2
1d	CH ₂ Ph	Br	15.0 ± 0.3	> 50	> 50
1e	CH ₃ (OC ₂ H ₄) ₃	I	> 50	> 50	> 50
3a	Et	NTf ₂	22.9 ± 1.7	> 50	> 50
3b	Et	Docusate	43.6 ± 0.6	> 50	> 50
3c	C ₁₀ H ₂₁	NTf ₂	1.3 ± 0.2	4.8 ± 1.2	7.0 ± 2.4
Doxorubicin			0.1 ± 0.04	0.5 ± 0.1	n.d

n.d – not determined

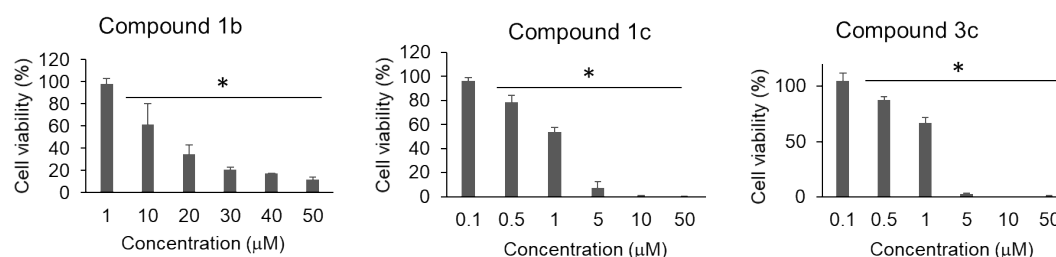


Figure 1. Anti-proliferative activity of **1b**, **1c** and **3c** in A2780 cell line after 48 h of incubation with increasing concentrations of each compound. Data normalized against the control (0.1 % (v/v) DMSO) and expressed as the mean \pm SEM of three independent assays. * p-value < 0.05 relative to control.

In fact, compound **1b**, with a methyl substitution at the R-position and iodide (I⁻) as counter ion, showed an IC₅₀ in A2780 cells of 12.5 ± 0.5 μ M (Table 2, Figure 1), and IC₅₀ > 50 μ M in both HCT116 and fibroblasts cell lines (Table 2, Figure S2). What is more, the length and structure of the aryl chain at the R-position seemed to have a relevant impact in the compound's antiproliferative activity. Indeed, **1c** and **3c** showed the lowest IC₅₀ of the series for all cell lines (Table 2, Figure 1, Figures S1-S3), and were the only compounds with an IC₅₀ < 50 μ M in HCT116 and fibroblasts (Table 2, Figure 1 and Figures S1-S3). Interestingly, the antiproliferative effect of compound **1d**, with CH₂Ph at the R-position, was similar to that of compound **1b** (Table 2, Figure 1 and Figure S1), with IC₅₀ in A2780 below that of compounds **1a**, **3a** and **3b**, with an ethyl group at the R-substitution. The polar coordinating group CH₃(OC₂H₄)₃ at R-substitution of compound **1e**, rendered no loss of cell viability for this compound towards the analyzed cell lines (Table 2, Figure S1, Figure S2). Despite the compounds show a higher IC₅₀ (at 48h) in A2780 and HCT116 cells when compared with the common chemotherapeutic agent doxorubicin (0.1 ± 0.04 μ M and 0.5 ± 0.1 μ M,

respectively), compound **1c** shows the most similar value (10x higher) (Table 2, Figure S4).

As described above, the relevance of the R-substitution is highlighted when comparing compounds with the same counter-ion, e.g. **3a** and **3c**. Despite similar observations are detected for compounds bearing I⁻ as counter-ion, **1b** stands-out as outlier as the methyl substitution in **1b** showed higher antiproliferative activity than the ethyl substitution in **1a** (Table 2). Since compounds **1b** and **1c** showed a considerable antiproliferative effect towards the A2780 ovarian cancer cell line (compound **1c** showing a selectivity index of 7.36) while **1b** presented no cytotoxicity against normal cells, the two compounds were selected for further biological analysis.

Mechanisms of cell death. To provide further insights towards the cell death mechanism induced by compounds **1b** and **1c** in A2780 cells, six different biological analysis were performed: i) apoptosis analysis by DNA staining with Hoechst 33258; ii) quantification of apoptosis based on double staining with annexin V conjugated with AlexaFluor488 and with propidium iodide (PI); iii) Trypan blue exclusion method (trypan blue stain is only internalized by cells with a compromised membrane - blue cells - non-viable [21]); iv) quantification of the apoptotic index through BAX/BCL-2 expression ratio for analysis of intrinsic apoptosis [22]; v) quantification of caspase 8 activity for the analysis of extrinsic apoptosis [23]; and vi) analysis of autophagy induced by compounds.

The staining of DNA with Hoechst 33258 allows the detection of nuclear modifications characteristic of apoptosis, such as chromatin condensation and nuclear fragmentation, that result in cell death [24]. After 48 h, nuclei of A2780 cells exposed to

IC₅₀ of compounds **1b** and **1c** revealed an increase in the number of nuclear modifications consistent with augmented apoptosis relative to control (Figure 2).

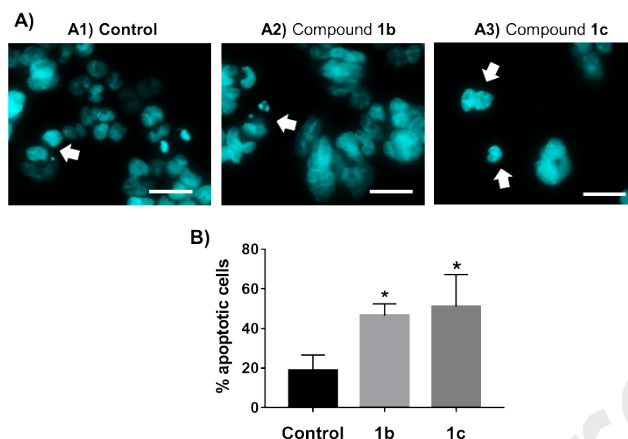


Figure 2. Apoptotic morphological changes in A2780 cells treated with compounds **1b** and **1c**. A) Representative images of A2780 cells incubated for 48 h with A1) 0.1 % (v/v) DMSO (control), A2) the IC₅₀ value at 48 h of compound **1b** and A3) the IC₅₀ value at 48 h of compound **1c**, and stained with Hoechst 33258 for observation of apoptotic events, pointed by white arrows, including chromatin condensation and nuclear fragmentation. Scale bar with 20 μ m. B) Percentage of apoptotic cells after incubation of A2780 cells for 48 h with compounds **1b** and **1c** and respective vehicle control. Values are represented as average \pm SD of at least three independent assays. * $p < 0.05$ relative to control.

For a more reliable quantification of cell death and to confirm the results in Figure 2, A2780 cells were incubated with IC₅₀ of compounds **1b** and **1c** and then double stained with Annexin V - AlexaFluor488 and PI (Figure 3). With this methodology, it is possible to distinguish between live cells (unstained), cells in early apoptosis (stained with annexin V - AlexaFluor488), cells in late apoptosis (stained with both fluorophores) and necrotic cells (only stained with PI). As observed in Figure 3, only a small increase in the number of apoptotic cells compared to control is observed when

A2780 cells were incubated for 48 h with the IC_{50} of compound **1c** and no difference compared to control when cells were incubated with the IC_{50} of compound **1b**. As expected DOXO was able to induce necrosis and apoptosis of A2780 cells (Figure 3). Considering the results for the positive control (DOXO) (Figure 3) and data from Figure 2, we were expecting to observe a higher level of cell death via apoptosis with Annexin V - AlexaFluor488 and PI double staining (Figure 3).

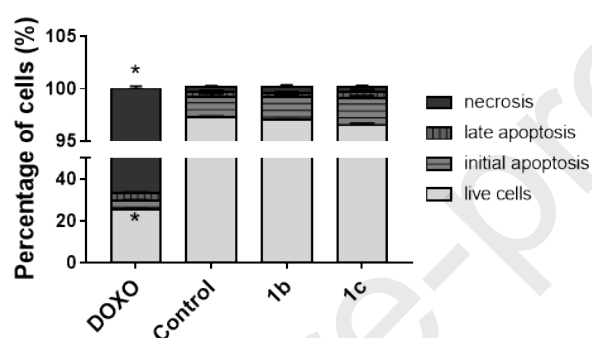


Figure 3: Quantification of apoptotic and necrotic A2780 cells exposed to compounds **1b** and **1c**. A2780 cells were incubated for 48 h with 0.1 % (v/v) DMSO (control), the IC_{50} concentration of doxorubicin (DOX), positive control of necrosis and apoptosis, or the IC_{50} concentration of compounds **1b** (12.5 μ M) and **1c** (1.1 μ M). Bars represent the average \pm SEM of at least three independent experiments. * $p < 0.05$ relative to control.

To clarify these results, we decided to confirm A2780 cell death induced by both compounds using another method - the Trypan blue exclusion method. For that, A2780 cells were exposed to the IC_{50} of each compound and to a concentration 10x higher and 10x lower the IC_{50} (Figure 4). Analysis of cell death was performed in cells that remained adherent (Figure 4) and in their respective supernatants (Figure 5).

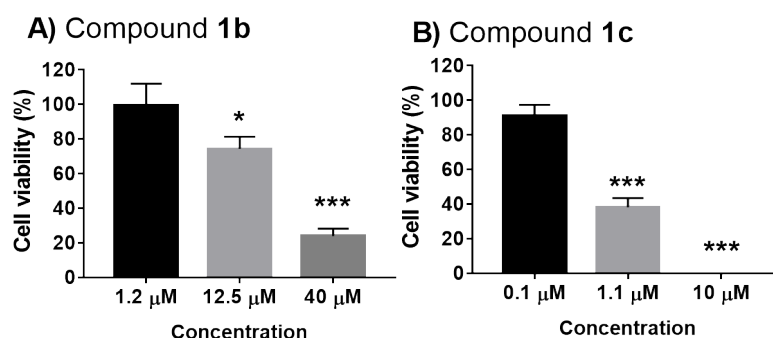


Figure 4: Viability of A2780 cells exposed to compounds **1b** (A) and **1c** (B). A2780 cells were incubated for 48 h with 0.1 % (v/v) DMSO (control), to the IC_{50} concentration of compounds **1b** (12.5 μ M) and **1c** (1.1 μ M), or to concentrations lower and higher than IC_{50} . Viability was normalized to the control and represented as the average \pm SD of three independent assays. * $p < 0.05$, *** $p < 0.001$ relative to control sample (0.1 % (v/v) DMSO).

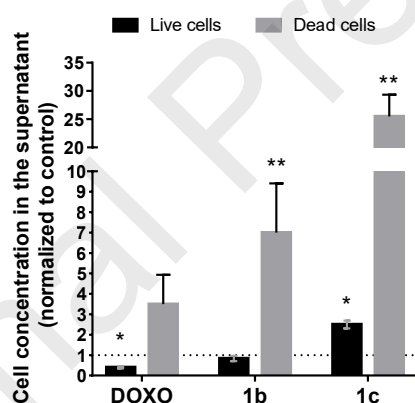


Figure 5. Concentration of A2780 cells in the supernatant after exposure to compounds **1b** and **1c**. A2780 cells were incubated for 6 h with 0.1 % (v/v) DMSO (Control), 4 μ M (10 x IC_{50}) of Doxorubicin (DOXO), 10 x IC_{50} of compound **1b**, and 10 x IC_{50} of compound **1c**. Cell concentration (cells/mL) of each sample was normalized to the cell concentration of the control. The value of the control is 1.0 ± 0.1 for live cells and 1.0 ± 0.6 for dead cells, represented as a black dotted line. Bars represent the average \pm SEM of three independent experiments. * p -value < 0.05 ** p -value < 0.001 comparing each concentration with respective control.

Considering the adherent cells, data showed a direct correlation to the results obtained with MTS analysis (Figure 1 and Figure 4), with one exception - when A2780 cells were exposed to 12.5 μ M of compound **1b** (Figure 4A), that accordingly to the MTS analysis should result in a decrease of 50% of viability and not 80% as observed in Figure 4A. However, since each method relies on different cellular properties (compromised membrane for Trypan blue exclusion assay and mitochondrial viability for the MTS), some discrepancies might occur. Still, both assays confirm the decrease of cell viability induced by the compounds.

Trypan blue analysis was also performed in cells in suspension - not adhered after exposure to the compounds. As observed in Figure 5, the concentration of live cells in the supernatant of A2780 culture treated with **1c** (black bars) increased 2.5 ± 0.2 times compared to the control. Interestingly, the concentration of cells stained with Trypan blue and considered as dead cells in the supernatants is very high (7 ± 2.4 higher than the control for cells treated with **1b**, and 25.5 ± 3.9 higher than control for cells treated with **1c** (Figure 5, gray bars)). The higher cell concentration in the supernatant of A2780 culture treated with **1b** and **1c** compared to the value obtained for cells treated with DOXO, might indicate that both compounds induce the loss of an adherent phenotype and cell death via detachment (Figure 5). These results indicate that apoptosis analysis via double staining with Annexin V - AlexaFluor488 and PI (Figure 3) might be underestimated due to cell detachment.

The apoptotic pathway is a highly regulated process that will ultimately lead to cell death [25-28]. Depending on the initial triggering signal, the apoptotic process can occur throughout two different pathways, the intrinsic or mitochondrial pathway is triggered by signals such as DNA damage or growth factors deprivation, and the extrinsic or death receptor pathway is mainly triggered by death-inducing signals [25-28]. Central to

the intrinsic apoptosis pathway are the anti-apoptotic BCL-2 family proteins [25-28]. In healthy cells, BCL-2 inhibit apoptosis through interaction with pro-apoptotic BAX protein which is located at the cytoplasm as monomer [25-28]. After an apoptotic signal, BAX insert in the mitochondrial outer membrane as homo-oligomer resulting in the permeabilization of the mitochondrial outer membrane and consequent dissipation of mitochondrial membrane potential ($\Delta\Psi_m$) [25-28]. The apoptotic index, that is the ratio of pro-apoptotic (BAX) and anti-apoptotic (BCL-2) proteins, is indicative of the cell susceptibility to the intrinsic apoptotic pathway [25-28].

Considering the results so far, the $\Delta\Psi_m$ of A2780 cells exposed to the IC_{50} of both compounds was analyzed (Figure 6). For this, a lipophilic cationic dye JC-1 with green fluorescence when in monomeric form (JC-1 monomer) and red fluorescence when in aggregated form (JC-1 aggregate) was used. The quantification of JC-1 monomer/aggregate fluorescence ratio (JC-1 ratio) give an indication of the $\Delta\Psi_m$ of the cell. In healthy cells, when the $\Delta\Psi_m$ is high, JC-1 accumulates in mitochondria and green / red fluorescence ratio is lower than 1 [29]. During both extrinsic and intrinsic apoptosis pathways, the mitochondrial membrane is compromised and a $\Delta\Psi_m$ dissipation occurs [25-28]. Figure 6 shows that a red to green shift is observed when cells are treated with both compounds, suggesting a depolarization of the $\Delta\Psi_m$. The $\Delta\Psi_m$ results suggest that the 80 % cell viability observed by the Trypan blue exclusion method (Figure 4) can be related to the presence of cells with depolarized mitochondrial membrane (Figure 6), but integral plasmatic membrane, which impacts the MTS assay. Indeed, after 48 h, the percentage of live A2780 cells incubated with **1b** was similar to the percentage of live cells in the control (Figure 3). Hence, at IC_{50} of compound **1b**, the cellular viability using the MTS assay should be lower than that determined via the Trypan Blue exclusion method.

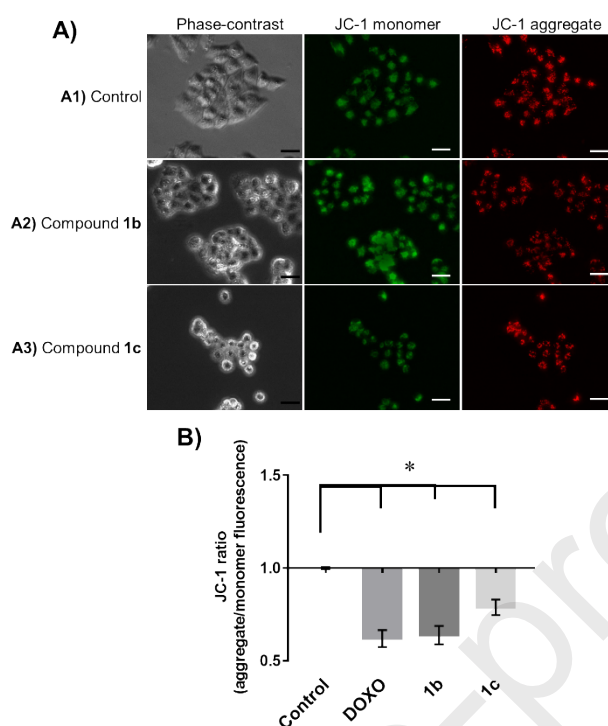


Figure 6. Mitochondrial membrane potential of A2780 cells treated with compounds **1b** and **1c**. A) A2780 cells were incubated for 48 h with A1) 0.1 % (v/v) DMSO, A2) IC₅₀ at 48 h compound **1b** and A3) IC₅₀ at 48 h compound **1c** and stained with JC-1. B) JC-1 monomer/aggregate ratio obtained after 48 h incubation of A2780 cells and quantification of JC-1 monomer and JC-1 aggregate fluorescence. Values were normalized to the JC-1 ratio of control cells (JC-1 ratio of control is 1). Bars represent the average \pm SEM of three independent experiments. * $p < 0.05$ relative to control sample.

The analysis of the apoptotic index through quantification of BAX and BCL-2 expression by western blot of total protein extract of A2780 exposed for 48 h to compounds **1b** and **1c**, followed by calculation of BAX/BCL-2 ratio, confirmed the results obtained in double staining apoptosis analysis (Figure 3), with compound **1c**

presenting BAX/BCL-2 ratios slightly higher, but not statistically significant, than control sample (Figure 7, Figure S5A and S5B with the entire western blot membranes). Interestingly, when we measure the apoptotic index of A2780 incubated for 18 h with compound **1c**, it was similar to the value obtained when cells were incubated with apoptosis inducer doxorubicin (Figure 8, Figure S6A and S6B with the entire western blot membranes), suggesting that the antiproliferative action of **1c** might be triggered earlier on time via the induction of intrinsic apoptosis.

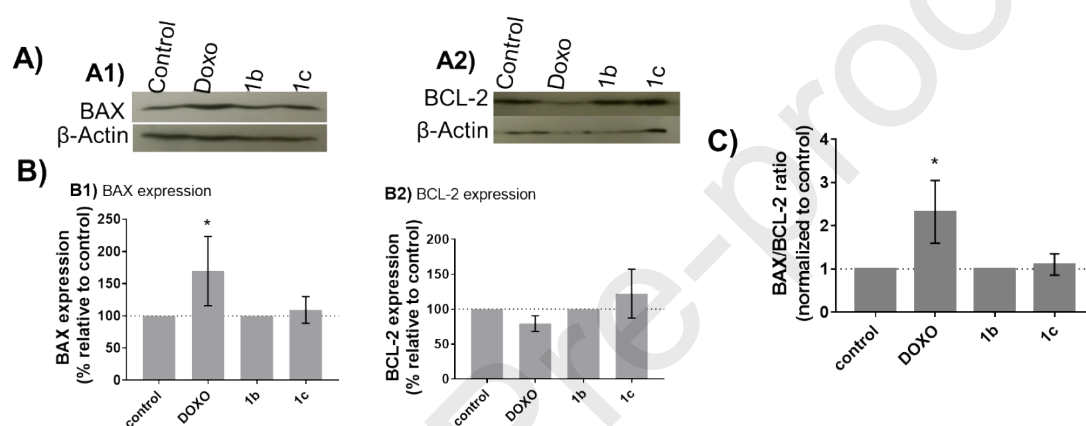


Figure 7. Expression of BAX and BCL-2 proteins in A2780 cells treated 48 h with compounds **1b** and **1c**. A) Western blot for quantification of A1) BAX and A2) BCL-2. Represented western blots correspond to 10 μ g total protein of A2780 incubated for 48 h with 0.1 % (v/v) DMSO (Control), 0.12 μ M doxorubicin (DOXO), the IC_{50} at 48 h of compound **1b** (12.5 μ M), or the IC_{50} at 48 h of compound **1c** (1.1 μ M). C) Protein expression of B1) BAX and B2) BCL-2 after normalization against β -actin and respective control (DMSO). The value of the control is 100%, represented as a grey dotted line. C) Apoptotic index of A2780 cells, calculated by BAX/BCL-2 ratio. The value of the control is 1, represented as a grey dotted line. Bars represent the average \pm SEM of three independent experiments. * p -value < 0.05 relative to control sample.

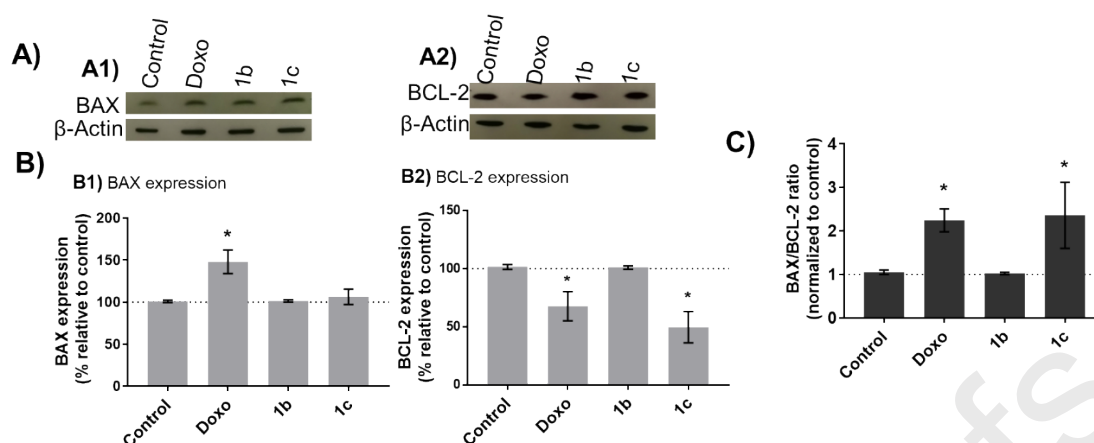


Figure 8. Expression of BAX and BCL-2 proteins in A2780 cells treated 18 h with compounds **1b** and **1c**. A) Western blot for quantification of A1) BAX and A2) BCL-2. Represented western blots correspond to 10 μ g total protein of A2780 incubated for 18 h with 0.1 % (v/v) DMSO (Control), 0.12 μ M doxorubicin (DOXO), the IC₅₀ at 48 h of compound **1b** (12.5 μ M), or the IC₅₀ at 48 h of compound **1c** (1.1 μ M). C) Protein expression of B1) BAX and B2) BCL-2 after normalization against β -actin and respective control (DMSO). The value of the control is 100%, represented as a grey dotted line. C) Apoptotic index of A2780 cells, calculated by BAX/BCL-2 ratio. The value of the control is 1, represented as a grey dotted line. Bars represent the average \pm SEM of three independent experiments. * p-value < 0.05 relative to control sample.

Caspase 8 is an initiator caspase central to the extrinsic apoptotic pathway, being activated by apoptotic stimuli from the plasmatic membrane [23]. After activation, caspase 8 cleave several molecules, such as downstream caspases, nuclear proteins, and plasma membrane and mitochondrial proteins [23]. To quantify the caspase 8 activity, the chromogenic substrate IEDT-*p*NA consisting in the IETD (Ile-Glu-Thr-Asp) peptide conjugated with the chromophore *p*-nitroanilide (*p*NA) is added to the total protein extract. As the substrate is cleaved by caspase 8, the *p*NA released is followed at 400

nm [30]. The caspase 8 activity of A2780 cells incubated for 18 h and 48 h with compounds **1b** and **1c** was measured. Similarly, at 48 h no difference compared to the control was observed (Figure S7), but after 18 h of exposition to compound **1b** the absorbance of *p*NA was 1.9 ± 0.4 times higher than control sample, suggesting the induction of apoptosis via the extrinsic pathway (Figure 9).

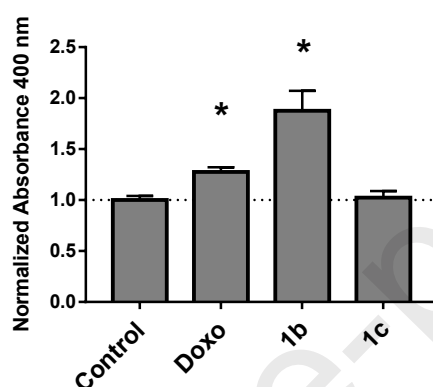


Figure 9. Caspase 8 activity in A2780 cells treated 18 h with compounds **1b** and **1c**. A2780 cells were incubated for 18 h with 0.1 % (v/v) DMSO (Control), 0.12 μ M Doxorubicin (DOXO), IC₅₀ at 48h of compound **1b** (12.5 μ M) or the IC₅₀ at 48 h of compound **1c** (1.1 μ M). Caspase 8 activity was quantified using the caspase 8 assay kit (Abcam). Absorbance at 400 nm values of each sample was normalized to the control. Bars represent the average \pm SEM of three independent experiments. * p-value < 0.05 relative to control.

To infer if **1b** and **1c** induce autophagy in A2780 cells, the culture was exposed to the IC₅₀ concentration of each compound and stained with an autophagic fluorescent dye (Abcam). According to the manufacturer, this dye is a cationic amphiphilic tracer that rapidly partition into cells and becomes highly fluorescent when incorporated in pre-autophagosomes, autophagosomes and autophagolysosomes. The fluorescence

quantification by flow cytometry revealed no differences between control sample (cells treated with 0.1 % (v/v) DMSO) and cells treated with each compound (Figure S8).

To further explore the mechanism triggered by compounds **1b** and **1c** that result in apoptosis induction and to correlate with data obtained so far, four other biological studies were performed, i) expression of E-cadherin, ii) incubation with 2',7'-bis(2-carboxyethyl)-5,6-carboxyfluorescein (BCECF-AM) to infer intracellular pH (pHi) and the state of plasma membrane [31-34]; and iii) mechanism of internalization of compounds and subcellular localization; iv) induction of reactive oxygen species (ROS).

The increased number of live cells in suspension when A2780 culture was exposed to compound **1c** (Figure 5, black bars) lead us to hypothesize the possibility of a decrease of E-cadherin expression and consequent cell detachment from the substrate. E-cadherin is the protein that connect epithelial cells at adherents' junctions, being vital for tissue homeostasis [35]. The western blot analysis of E-cadherin expression in A2780 treated for 48 h with IC₅₀ of compounds **1b** and **1c** revealed a decrease of E-cadherin protein expression (Figure 10 and Figure S9, with the entire western blot membranes) that correlates with the loss of cell adhesion (Figure 5) and with the trigger of an apoptotic process (Figures 2, 6 and 8) [36].

On the other side, the decreased expression of E-cadherin is a hallmark of epithelial-to-mesenchymal transition in cancer cells and is accompanied by extrinsic apoptosis attenuation (Figure S7) [37]. When looking to A2780 cells exposed to IC₅₀ of the common antitumor drug doxorubicin a very high decrease of E-cadherin expression is observed [38] correlating with the observed intrinsic apoptosis (Figure 8).

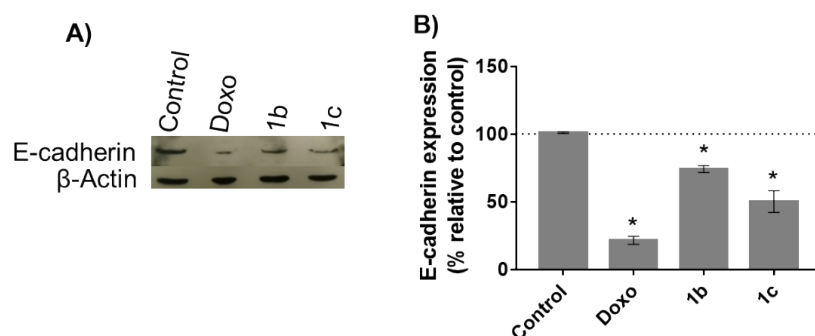


Figure 10. Expression of E-cadherin protein in A2780 cells treated 18 h with compounds **1b** and **1c**. A) Western blot for quantification of expression for E-cadherin. Represented Western-blot correspond to 50 μ g total protein for CDH1 of A2780 cells incubated 18 h with 0.1 % (v/v) DMSO (vector control of compounds), 0.4 μ M doxorubicin (DOXO) or the IC₅₀ at 48 h of compound **1b** (12.5 μ M) or compound **1c** (1.1 μ M). B) Percentage of protein expression of E-cadherin after normalization against β -actin and respective control. The value of control is 100 % represented as a dotted line for comparison. Bars represent average \pm SEM of three independent experiments. * p-value < 0.05. relative to control.

During apoptosis, intracellular pH (pHi) might increase [33, 34]. In order to analyse changes in pHi after exposure to both compounds, cells were incubated with BCECF-AM, a non-charged molecule that enter cells, and once inside, the intracellular esterases cleave the ester bond releasing BCECF whose fluorescence increase as the pHi increases [39]. It should be noted that due to the passive diffusion of BCECF-AM into the cells, the loss of fluorescence intensity can also occur in cells with compromised membranes [31, 32]. The fluorescence of A2780 cells treated with compounds **1b** and **1c** was measured after 3 h, 6 h, 18 h and 48 h incubation with BCECF-AM. An increased fluorescence was detected when A2780 cells were incubated for more than 18 h with doxorubicin and both compounds **1b** and **1c** (Figure S10),

suggesting an alcalinization of the pHi, possibly due to apoptosis [33, 34]. A transient fluorescence increase is also observed when A2780 cells were incubated for 3 h with compound **1b**, suggesting a pHi alteration that might be promoted by the compound entry into cells (Figure S10), but not observed with compound **1c**. This might indicate that both compounds enter cells via distinct mechanisms. In order to confirm this observation and taking the fact that compounds **1b** and **1c** exhibited a blue fluorescence upon excitation at 340-380 nm in an inverted fluorescence microscope, it was possible to gather information concerning their internalization and accumulation in cells over time.

The presence of compounds **1b** and **1c** in cells after 1 hour of incubation was perceived by an increased fluorescence in treated relative to untreated cells (Figure S11).

Remarkably, the fluorescence in cells treated with compound **1b** kept increasing with time (3 h > 1 h) (Figure S11A, S11D), whereas for compound **1c** the fluorescence levels at 1 h and 3 h were equivalent (Figure S11B, S11D). This higher concentration of compound (10x IC₅₀) was needed to ensure the visualization of the compound inside the cell by fluorescence microscopy. After 3 h incubation in the presence of 10x the IC₅₀ of compound **1b** exhibited a fluorescence signal along the cytoskeleton stain (Figure S12A) with higher fluorescence intensity co-localizing with vesicles near the plasma membrane (Figure S12B). Interestingly, morphological alterations can be observed for A2780 cells incubated with 10x the IC₅₀ of compound **1c** for 3 h (Figure S13 and Figure S14). Indeed, cells treated with compound **1c** seem to be rounder with a smaller cytoplasm (Figure S13 and Figure S14). Counterstaining of both the cytoskeleton and nucleus allowed to visualize the distribution of the compound all over the cell with blebbing at spots (Figure S13B, white arrow). What is more, one can clearly visualize cells with blue fluorescence but no cytoplasmic staining, suggesting compound

internalization by the cell and cytoskeleton damage (Figure S13B, red arrow). A closer analysis to the cell morphology when A2780 cells were treated with compound **1c** (Figure S13) reveals several events in line with oncosis. In this programmed cell death, a membrane injury causes the leak of ions and water, resulting in cell swelling without increased cell membrane permeability, altering cell shape and volume, which can be observed by the formation of cytoplasmic blebs [40, 41]. As the oncotic process continues, the membrane permeability increases continuously, other alterations occur, such as chromatin clumping, dilatation of ER and Golgi, mitochondrial condensation and significant alterations of the cytoskeleton [41]. At later stages, cells will continue to round up and detach from the substrate [40, 41]. All the results relating to the cell effects of compound **1c** agree with early oncotic events: the round up and blebbing of cells in monolayer is easily observed when the ovarian cancer cells were incubated with compound **1c** and stained with Phalloidin (Figure S12B), where one unstained cell may be observed (Figure S12B, red arrow) suggesting cytoskeleton alterations in agreement with the literature [42].

In resume, compound **1b** shows an increased internalization over time (Figure S11A), a small but significant decrease of internalization at 4 °C (Figure S15A), and co-localization with vesicles located near the cell surface (Figure S12). Altogether, these data suggest that compound uptake occurs by passive diffusion and possibly by low level endocytosis. These observations are in line with results obtained for intracellular pH of A2780 cells incubated with **1b**, where a transient pH increase was observed after 3 h incubation (Figure S10).

Next, we evaluated whether the uptake of these compounds was due to passive or active transport, by assessing internalization at 37 °C and 4 °C - at 4 °C the energy balance of the cell is severely diminished and active transport decreases. Incubation at 4

°C revealed a slight decrease of compound **1b** internalization when compared to 37 °C (Figure S15A, Figure S15C1) but an accentuated decreased of compound **1c** internalization (Figure S15B, Figure S15C2). These results suggest that internalization of compound **1b** relies on passive diffusion, while compound **1c** might also permeate the cell membrane via an active uptake mechanism [43, 44]. This difference might be attributed to the different size of the R-substitution.

Due to the cell damages induced by ROS, such as DNA strand breaks or membrane blebbing, the induction of oxidative stress is intrinsically related to apoptosis [45]. The induction of ROS by both compounds was evaluated using 2,7-dichlorodihydrofluorescein diacetate (H₂DCF-DA) which, after de-acetylation and oxidation by peroxides present in cells, forms the highly fluorescent 2'7'dichlorofluorescein (DCF). A2780 cells exposed to IC₅₀ of compounds **1b** and **1c** present levels of ROS similar to the control (Figure S16). These data suggest that both compounds are not able to induce the production of ROS and, thus, oxidative stress.

The accumulation of the compound **1c** in the cytoplasm and not in the nuclei (Figure S12), coupled with the absence of oxidative stress (Figure S16), suggest a different mechanism of cytotoxicity for compound **1b** to those of anthracyclines commonly used in chemotherapy, such as doxorubicin [46]. The IC₅₀ of compound **1b** in colorectal cancer cells and normal fibroblasts is greater than 50 μM (Table 2). However, the high fluorescence in HCT116 cells incubated with the **1b** (Figure S11A) suggests internalization of the compound. The cytotoxicity of compound **1b** in A2780 cells, with low impact to healthy fibroblasts, might be associated to intrinsic characteristics of the ovarian cancer cells, making this compound suitable for ovarian cancer therapy.

3. Conclusion

The antiproliferative activity of hetero-arylidene-9(10*H*)-anthrone derivatives seemed to be mainly reliant on the R-substitution of the cation counterpart and in a low scale in the counter anion. Moreover, the nature of the R-substitution showed to be relevant for cytotoxicity with compounds with a long alkyl chain as C₁₀H₂₁ showing the highest cytotoxicity in all cell lines, including normal primary dermal fibroblasts. Based on the index selectivity towards ovarian cancer cells, two compounds containing the same counter anion (I⁻) and distinct R-substitution were selected for further cytotoxicity analysis. Interestingly, the cellular uptake and mechanisms of cytotoxicity of compounds with methyl- or C₁₀H₂₁ substitutions at the R-position, compounds **1b** and **1c**, respectively, were different and distinct between each other and from those described for anthracyclines used in chemotherapy, such as doxorubicin. Our data provide interesting clues on the cytotoxic mechanisms affecting A2780 cells induced by compounds **1b** and **1c**. As observed in the analysis of anti-proliferative activity of the compounds, the R- substitution is preponderant for the compound's internalization and mechanism of cell death induced by the hetero-arylidene-9(10*H*)-anthrone derivatives. The evaluation of the presence of apoptotic events in the nuclei, and decreased monomer/aggregate JC-1 ratio after 48 h, and increased caspase-8 activity after 18 h suggest that compound **1b** induces extrinsic apoptosis.

Despite the only difference resides in the R-substitution from a methyl group in **1b** to an aliphatic hydrophobic chain, C₁₀H₂₁, in **1c**, the mechanism of cell uptake and cytotoxicity of compound **1c** showed to be different to those of compound **1b**. In fact, following 1 h and 3 h incubation with compound **1c**, A2780 cells show similar fluorescence intensity but a dramatic fluorescence decrease was observed when A2780 was incubated at 4 °C, which strongly indicates passive transport of the compound. As

for compound **1b**, the accumulation of compound **1c** in the cytoplasm and lack of oxidative stress suggest a toxicity mechanism different to that of doxorubicin.[46] The presence of nuclei modifications characteristic of apoptosis, such as chromatin condensation, alteration of the mitochondrial membrane potential after 48 h, and increased apoptotic index after 18 h is suggestive of induced intrinsic apoptosis. Nevertheless, the increased concentration of live and dead cells at the supernatant when A2780 cell culture was exposed to **1c**, the roundup and blebbing of cells and phalloidin unstained cells does not exclude the possibility of oncosis. In fact, it is reported that apoptosis and oncosis are closely related mechanisms, apoptotic cells may undergo oncosis due to energetic requirements [23].

Despite compound **1b** and **1c** show a higher IC_{50} in A2780 cell line when compared to common chemotherapeutic drug - doxorubicin, the high selectivity index, and apoptosis induction of both compounds, compared with doxorubicin that also induces necrosis to the cells,[38] might be of interest for further studies due to the distinct mechanism of action. Indeed, the induction of ROS is one of the most deleterious mechanism of action attributed to doxorubicin, resulting in cardiotoxic side effects and limiting the dose and length of treatment in cancer patients.

4. Experimental Section

MATERIALS AND METHODS. All the reagents and solvents were obtained commercially, and these were used without further purification. The solvents used were dried using current laboratory techniques. Thin layer chromatography (TLC) was carried out on aluminium backed Kieselgel 60 F254 silica gel plates (Merck). Plates were visualized by UV light (254 and/or 366nm). Preparative layer chromatography (PLC) was performed on Merck Kieselgel GF 254 silica gel plates

with a thickness of 0.5 mm or 1 mm. Column chromatography were carried out on silica gel Kieselgel 60 (Merck), 70 - 230 mesh particle size as stationary phase, in normal phase chromatography. Ultraviolet spectroscopy (UV) was recorded on a Thermo Corporation spectrophotometer, Helius γ , on quartz cell support. Absorption spectrum measurements were made in the range of 190 to 320 nm. ^1H and ^{13}C NMR spectra were recorded on a Bruker ARX400 at 400 and 100 MHz, respectively. Chemical shifts are reported in parts per million (ppm, δ units). The following NMR abbreviations are used: s = singlet, d = doublet, t = triplet, q = quartet, m = multiplet, brs = broad singlet. HPLC-MS-ESI was acquired on a Agilent 1200 Series LC with quaternary pump, ALS, TCC, DAD, and Agilent G6130B LC/MSD with API-ES source. High Resolution Mass spectra (MS) using the EI-TOF technique were obtained from Unidade de Masas e Proteómica, the University of Santiago de Compostela, Spain.

General procedure for the preparation of imidazolium salts (2a-e): In a round bottom flask equipped with magnetic stir bar was added 1,2-dimethylimidazol in dry THF to make a 0.55 M solution and the corresponding alkyl halide (1 to 1.2 equiv). The reaction mixture was stirred at reflux under N_2 atmosphere until the total consumption of the 1,2-dimethylimidazol was verified. This monitoring was carried out by TLC, in an eluent of MeOH/dichloromethane (5:95). The product as formed began to precipitate from the reaction medium and after terminus of the reaction the product was filtered and used as so.

Procedure for the preparation of 3-{2-[2-(2-methoxyethoxy)ethoxy]ethyl}-1,2-dimethyl-1*H*-imidazol-3-ium iodide (2e): To a solution of triethylene glycol monomethyl ether (3.0×10^{-3} mol) in THF (20 mL) were added triphenylphosphine (0.97 g, 3.7×10^{-3} mol, 1.2 equiv) and imidazole (0.61 g, 9.0×10^{-3} mol, 3.0 equiv) The

mixture was stirred under nitrogen atmosphere at room temperature for 3 minutes. Then the reaction mixture was cooled to $-20\text{ }^{\circ}\text{C}$ and I_2 (1.01 g, 3.98×10^{-3} mol, 1.2 equiv) was added. After stirring at this temperature for 15 minutes the cooling bath was removed, and the mixture stirred at room temperature for 2 h until the total consumption of triethylene glycol monomethyl ether was verified. This monitoring was carried out by TLC, in an eluent of hexane and ethyl acetate (8:2) (spray reagent: phosphomolybdic acid solution). The reaction was quenched at $0\text{ }^{\circ}\text{C}$ with an aqueous saturated solution of NaHCO_3 (20 mL). The reaction mixture was filtered through out celite several times until all white precipitate formed was removed. The aqueous phase was extracted with diethyl ether and the combined organic phases were washed with a saturated solution of $\text{Na}_2\text{S}_2\text{O}_5$ (20 mL) and brine, dried over Na_2SO_4 anhydrous, filtered and evaporated. The residue was purified by chromatography on silica gel using as eluent a mixture of hexane and ethyl acetate (8:2), affording 3-{2-[2-(2-methoxyethoxy)ethoxy]ethyl} iodide (0.58g, 77%) as a yellow oil. In a round bottom flask equipped with magnetic stir bar was added 3-{2-[2-(2-methoxyethoxy)ethoxy]ethyl} iodide (0.57g, 2.1×10^{-3} mol, 1.4 equiv) and the 1,2-dimethylimidazol (0.14g, 1.5×10^{-3} mol) in dry THF. The reaction mixture was stirred and refluxed for 122 h under nitrogen atmosphere until the total consumption of the 1,2-dimethylimidazol was verified. This monitoring was carried out by TLC, in an eluent of dichloromethane/MeOH (95:5) (spray reagent: Dragendorff-Munier solution). The reaction mixture was evaporated and washed with diethyl ether, affording 3-{2-[2-(2-methoxyethoxy)ethoxy]ethyl}-1,2-dimethyl-1*H*-imidazol-3-ium iodide (**2e**) (0.40g, 75%) as a yellow oil; $^1\text{H NMR}$ (CDCl_3 , 400 MHz) δ : 7.72 (d, $J = 2.0$ Hz, 1H, H-4), 7.49 (d, $J = 2.4$ Hz, 1H, H-5), 4.48 – 4.43 (t, 2H, $J = 4.8$ Hz, H-1''a), 3.94 (s, 3H, H-6), 3.89 – 3.86 (t, 2H, 4.8 Hz, H-2''a), 3.61 – 3.59 (m, 2H, CH_2),

3.56 – 3.55 (m, 4H, 2xCH₂), 3.53 – 3.48 (m, 2H, 2xCH₂), 3.35 (s, 3H, CH₃), 2.80 (s, 3H, CH₃) ppm. ¹³C NMR (CDCl₃, 100 MHz) δ: 144.86 (C-2), 122.56 (CH), 121.94 (CH), 71.81 (CH₂), 70.38 (CH₂), 70.26 (2xCH₂), 69.30 (CH₂), 58.98 (OCH₃), 49.18 (CH₂), 36.44 (CH₃-6), 11.62 (CH₃-7) ppm. IR ν_{max} (cm⁻¹): 2897 (vs C-H aliphatic), 1095 (ν_{as} C-O-C), 1586 (w, C=N). HRMS (ESI-TOF) m/z: [M + H]⁺ Calc for C₁₂H₂₃N₂O₃ 243.1706, found 243.1703.

General procedure for the preparation hetero arylidene-9(10H)-anthrone

(1a-e): In a round bottom flask equipped with magnetic stir bar was added the imidazolium salt **2** (0.6 mmol) and Cs₂CO₃ (1.2 equiv) in dry THF (5 mL). The reaction mixture was stirred at room temperature for 1 h and then 9-anthracenecarboxaldehyde (1 equiv) was added. The reaction mixture was stirred at room temperature until the total consumption of the aldehyde was verified (7 to 8 days). This monitoring was carried out by TLC, in an eluent of dichloromethane/MeOH (85:15). The reaction mixture was evaporated under reduced pressure, the crude product was washed with diethyl ether to remove less polar compounds and then washed with water to remove any remaining base or imidazolium salt. The title compound was obtained by column chromatography using dichloromethane/MeOH (85:15) as eluent.

1,3-Dimethyl-2-[[10-oxoanthracen-9(10H)-ylidene]methyl]-1H-imidazol-3-ium iodide (1b). Yellow / Brown solid (14%); mp: >280 °C. ¹H NMR (CDCl₃, 400MHz) δ: 8.31 (t, *J* = 7.6 Hz, 2H, H-4' and H-5'), 8.25 (d, *J* = 8.0 Hz, 1H, H-1'), 7.76 (t, *J* = 7.6 Hz, 1H, H-7'), 7.73 (br s, 2H, H-4 and H-5), 7.67 – 7.58 (m, 2H, H-6' and H-3'), 7.58 (s, 1H, H-10''), 7.49 (t, *J* = 7.6 Hz, 1H, H-2'), 6.68 (d, *J* = 7.6 Hz, 1H, H-8'), 3.68 (s, 6H, 2x CH₃) ppm. ¹³C NMR (CDCl₃, 100MHz) δ: 183.20 (C-10'), 145.97 (C-1'a), 142.92 (C-2), 136.35 (C-8'a), 134.30 (CH-7'), 134.15 (C-4'a), 133.70

(CH-2'), 131.83 (C-9'), 131.35 (CH-6'), 130.99 (CH-3'), 130.56 (C-5'a), 128.64 (CH-5'), 127.62 (CH-1'), 125.33 (CH-4'), 125.22 (CH-8'), 124.35 (CH-4 and CH-5), 109.32 (CH-10''), 36.94 (2x CH₃) ppm. ESI-MS (*m/z*) (+): 301.1 [M]⁺; ESI-MS (*m/z*) (-): 126.9 [I]⁻. IR ν_{\max} (cm⁻¹): 2925 (m, ν_{as} C-H), 2849 (w, ν_{s} C-H), 1666 (m, C=O), 1590 (w, C=N), 1313 (w, C-N). HRMS (ESI-TOF) *m/z*: [M + H]⁺ Calc for C₂₀H₁₇N₂O 301.1338, found 301.1335.

3-Decyl-1-methyl-2-{{10-oxoanthracen-9(10H)-ylidene}methyl}-1H-imidazol-3-ium iodide (1c). Red solid (61%); mp: 169-176 °C. ¹H NMR (CDCl₃, 400MHz) δ : 8.36 (d, *J* = 8.0 Hz, 1H, H-4'), 8.31 (d, *J* = 8.0 Hz, 1H, H-1'), 8.26 (d, *J* = 8.0 Hz, 1H, H-5'), 7.92 (d, *J* = 2.0 Hz, 1H, H-4), 7.76 (t, *J* = 7.2 Hz, 1H, H-7'), 7.68 (s, 1H, H-10''), 7.67 (d, *J* = 2.0 Hz, 1H, H-5), 7.66 – 7.57 (m, 2H, H-3' and H-6'), 7.47 (t, *J* = 8.0 Hz, 1H, H-2'), 6.63 (d, *J* = 8.0 Hz, 1H, H-8'), 3.96 (dd, *J* = 6.4 and 15.2 Hz, 2H, H-1'''), 3.67 (s, 3H, CH₃), 1.84 – 1.69 (m, 1H, H-2'''), 1.59-1.49 (m, 1H, H-2'''), 1.19 – 1.30 (m, 14H, 7 X CH₂), 0.81 (t, *J* = 6.8 Hz, 3H, H-10''') ppm. ¹³C NMR (CDCl₃, 100MHz) δ : 183.13 (C-10'), 145.30 (C-1'a), 142.26 (C-2), 136.38 (C-8'a), 134.26 (CH-7'), 134.09 (C-4'a), 133.51 (C-2'), 131.87 (C-9), 131.22 (CH-6'), 130.89 (CH-3'), 130.49 (C-5'a), 128.64 (CH-5'), 127.56 (CH-1'), 125.39 (CH-4'), 125.11 (CH-8'), 124.72 (CH-4), 122.52 (CH-5), 109.79 (CH-10''), 49.75 (CH₂-1'''), 36.82 (CH₃), 31.82 (CH₂), 29.41 (CH₂), 29.37 (CH₂), 29.33 (CH₂), 29.21 (CH₂), 28.92 (CH₂), 26.42 (CH₂), 22.65 (CH₂), 14.12 (CH₃-10''') ppm. ESI-MS (*m/z*) (+): 427.3 [M]⁺; ESI-MS (*m/z*) (-): 126.9 [I]⁻. IR ν_{\max} (cm⁻¹): 3050 (w, C-H Ar.), 2925 (m, ν_{as} C-H) 2853 (w, ν_{s} C-H), 1662 (s, C=O), 1591 (m, C=N), 1314 (m, C-N). HRMS (ESI-TOF) *m/z*: [M + H]⁺ Calc for C₂₉H₃₅N₂O 427.2740, found 427.2744.

3-Benzyl-1-methyl-2-{{10-oxoanthracen-9(10H)-ylidene}methyl}-1H-imidazol-3-ium iodide (1d). Yellow/Orange solid (η =38%); mp: 129-137 °C. ¹H

NMR (CDCl₃, 400MHz) δ : 8.52 (d, J = 8.0 Hz, 1H, H-4'), 8.28 – 8.21 (m, 2H, H-1' and H-5'), 8.05 (br s, 1H, H-4), 7.91 (s, 1H, H-10''), 7.80 (m, 2H, H-5 and H-7'), 7.62 (t, J = 7.6 Hz, 1H, H-3'), 7.52 (t, J = 7.6 Hz, 1H, H-6'), 7.44-7.42 (m, 2H, H-2''' and H-6'''), 7.25-7.20 (m, 4H, H-2', H-3''', H-4''' and H-5'''), 6.15 (d, J = 8.0 Hz, 2H, H-8'), 5.71 (d, J = 14.4 Hz, 1H, CH₂Ph), 5.54 (d, J = 14.8 Hz, 1H, CH₂Ph), 3.33 (s, 3H, CH₃) ppm. ¹³C NMR (CDCl₃, 100MHz) δ : 183.37 (C-10'), 144.95 (C-1'a), 142.82 (C-2), 136.59 (C-8'a), 134.44 (C-7'), 134.28 (C-4'a), 133.17 (CH-2'), 132.83 (C-1'''), 131.87 (C-5'a), 131.01 (CH-9'), 130.80 (CH-6'), 130.52 (C-3'), 129.52 (C), 129.43 (CH-2''' and CH-6'''), 129.38 (CH-3''' and CH-5'''), 128.54 (CH-5'), 127.53 (CH-1'), 125.62 (CH-4'), 124.78 (CH-8'), 124.13 (CH-5), 123.49 (CH-4), 110.34 (CH-10''), 53.60 (CH₂Ph), 35.98 (CH₃) ppm. ESI-MS (m/z) (+): 377.2 [M]⁺; ESI-MS (m/z) (-): 125.0 [⁷⁹Br + HCOOH]⁻, 127.0 [⁸¹Br + HCOOH]⁻. IR ν_{\max} (cm⁻¹): 3059 (w, C-H Ar.), 3022 (w, C-H Ar.), 2920 (w, ν_{as} C-H), 1666 (m, C=O), 1590 (w, C=N), 1313 (C-N). HRMS (ESI-TOF) m/z : [M + H]⁺ Calc for C₂₆H₂₁N₂O 377.1648, found 377.1651.

3-{2-[2-(2-methoxyethoxy)ethoxy]ethyl}-1-methyl-2-{[10-oxoanthracen-9(10H)-ylidene]methyl}-1H-imidazol-3-ium iodide (1e). Dark red solid (η =22%); mp: 125-138 °C. ¹H NMR (CDCl₃, 400MHz) δ : 8.38 (d, J = 8.0 Hz, 1H, H-4'), 8.33 (d, J = 7.6 Hz, 1H, H-5'), 8.28 (d, J = 7.6 Hz, 1H, H-1'), 8.08 (d, J = 2.0 Hz, 1H, H-4), 7.78 (t, J = 7.2 Hz, 1H, H-7'), 7.76 (s, 1H, H-10''), 7.67 - 7.59 (m, 3H, H-3', H-5 and H-6'), 7.50 (t, J = 7.6 Hz, 1H, H-2'), 6.78 (d, J = 7.6 Hz, 1H, H-8'), 4.60 – 4.51 (m, 1H, H-1'''a), 4.40 (m, 1H, H-1'''a), 4.07 – 3.97 (m, 1H, H-2'''a), 3.85 – 3.75 (m, 1H, H-2'''a), 3.62 – 3.48 (m, 6H, 3 x CH₂), 3.43 – 3.40 (4, 7H, 2 x CH₂ and CH₃), 3.28 (s, 3H, OCH₃) ppm. ¹³C NMR (CDCl₃, 100MHz) δ : 183.37 (C-10'), 145.39 (C-1'a), 143.20 (C-2), 136.57 (C-8'a), 134.32 - 134.29 (CH-7' and C-4'a), 133.57 (CH-

2'), 131.91 (C9'), 131.18 (CH-6'), 130.90 (CH-3'), 130.59 (C-5'a), 128.61 (CH-5'), 127.61 (CH-1'), 125.54 (CH-8'), 125.44 (CH-4'), 123.96 (CH-5), 123.83 (CH-4), 110.19 (CH-10''), 71.91 (CH₂-2''c), 70.46 (CH₂), 70.41 (CH₂), 70.28 (CH₂), 68.93 (CH₂-2''a), 59.07 (OCH₃), 50.04 (CH₂-1''a), 36.26 (CH₃) ppm. ESI LC-MS (*m/z*): 433.2 [M]⁺. IR ν_{\max} (cm⁻¹): 3090 (w, C-H Ar.), 2929 (w, ν_{as} C-H), 2867 (m, ν_{s} C-H), 1671 (w, C=O), 1591 (m, C=N), 1314 (w, C-N), 1100 (w, ν_{as} C-O-C). HRMS (ESI-TOF) *m/z*: [M + H]⁺ Calc for C₂₆H₂₉N₂O₂ 433.2121, found 433.2122.

General procedure for ion exchange with LiNTf₂ [17]. To a solution of 3-ethyl-1-methyl-2-{{[10-oxoanthracen-9(10*H*)-ylidene]methyl}-1*H*-imidazol-3-ium iodide (**1a**) (0.026g, 5.7x10⁻⁵mol) or 3-decyl-1-methyl-2-{{[10-oxoanthracen-9(10*H*)-ylidene]methyl}-1*H*-imidazol-3-ium iodide (**1c**) (0.025g, 0.045mmol) in H₂O (1mL) was added dropwise a solution of LiN(Tf)₂ (1.1equiv) in H₂O (1mL). The reaction mixture was stirred at room temperature for 24h. The product precipitate with time, the solvent was decanted and the product washed with water.

3-Ethyl-1-methyl-2-{{[10-oxoanthracen-9(10*H*)-ylidene]methyl}-1*H*-imidazol-3-ium bistriflimide (3a**)**. Yellow oil (η =72%, 50% over two steps). ¹H NMR (CDCl₃, 400MHz) δ : 8.31 (d, *J* = 8.0 Hz, 1H, H-4'), 8.27 (t, *J* = 7.6 Hz, 2H, H-5' and H-1'), 7.77 (t, *J* = 7.6 Hz, 1H, H-7'), 7.67 - 7.61 (m, 3H, H-3', H-4 and H-5), 7.47 (t, *J* = 7.6 Hz, 1H, H-6'), 7.45 (s, 1H, H-10''), 6.61 (d, *J* = 7.6 Hz, 1H, H-8'), 4.08 – 3.96 (m, 2H, CH₂), 3.60 (s, 3H, CH₃), 1.37 (t, *J* = 7.2 Hz, 3H, CH₃) ppm. ¹⁹F NMR (CDCl₃, 376 MHz) δ : -78.80 (CF₃) ppm. ESI-MS (*m/z*) (+): 315.2 [M]⁺; ESI-MS (*m/z*) (-): 280.0 [NTf₂]⁻.

3-Decyl-1-methyl-2-{{[10-oxoanthracen-9(10*H*)-ylidene]methyl}-1*H*-imidazol-3-ium bistriflimide (3c**)**. Orange / red oil (η =89%, 62% over two steps). ¹H NMR (CDCl₃, 400MHz) δ : 8.34 (d, *J* = 8.0 Hz, 1H, H-4'), 8.30 (d, *J* = 7.6 Hz, 1H, H-5'),

8.21 (d, $J = 7.6$ Hz, 1H, H-1'), 7.78 (t, $J = 7.2$ Hz, 1H, H-7'), 7.68 - 7.59 (m, 3H, H-3', H-5 and H-6'), 7.50-7.47 (m, 2H, H-2' and H-4), 7.35 (s, 1H, H-10''), 6.62 (d, $J = 7.6$ Hz, 1H, H-8'), 3.89 (t, $J = 7.2$ Hz, 2H, H-1'''), 3.58 (s, 3H, CH₃), 1.77 - 1.72 (m, 1H, H-2'''), 1.60 - 1.54 (m, 1H, H-2'''), 1.22 - 1.16 (m, 14H, 7 x CH₂), 0.84 (t, $J = 6.4$ Hz, 3H, H-10''') ppm. ¹³C NMR (CDCl₃, 100MHz) δ : 183.17 (C-10'), 145.95 (C), 145.87 (C), 142.23 (C), 136.40 (C), 134.29 (CH), 134.25 (CH), 134.05 (C), 133.60 (CH), 131.90 (CH), 131.40 (C), 131.06 (CH), 130.61 (C), 128.74 (CH), 127.71 (CH), 127.32 (CH), 125.06 (CH), 124.95 (CH), 124.48 (CH), 122.39 (CH), 108.61 (CH), 49.54 (CH₂), 36.14 (CH₃), 31.87 (CH₂), 29.44 (CH₂), 29.33 (CH₂), 29.29 (CH₂), 29.26 (CH₂), 28.92 (CH₂), 26.39 (CH₂), 22.70 (CH₂), 14.17 (CH₃) ppm. ¹⁹F NMR (CDCl₃, 376 MHz) δ : -78.77 (CF₃). IR ν_{\max} (cm⁻¹): 3080 (w, C-H Ar.), 3049 (w, C-H Ar.), 2929 (m, ν_{as} C-H), 2857 (m, ν_{s} C-H), 1666 (m, C=O), 1595 (m, C=N), 1350 (m, ν_{as} O=S=O), 1193 (s, C-F), 1140 (m, ν_{s} O=S=O).

Procedure for ion exchange with docusate sodium salt. In a round flask equipped with a magnetic stir bar were added docusate sodium salt (0.032g, 6.8×10^{-5} mol, 1.1 equiv), Amberlyst® 15 (0.050g) and 3mL of H₂O. The reaction mixture was stirred at room temperature for 24h. The reaction mixture was filtered in order to remove the resin and then to the solution was added 3-ethyl-1-methyl-2-{{10-oxoanthracen-9(10*H*)-ylidene]methyl}-1*H*-imidazol-3-ium iodide (**1a**) (0.027g, 6.1×10^{-5} mol). The stirring was continued for 115 h and then decanted, and the solid product was washed with water.

3-Ethyl-1-methyl-2-{{10-oxoanthracen-9(10*H*)-ylidene]methyl}-1*H*-imidazol-3-ium docusate (3b**).** Yellow oil ($\eta = 25\%$, 18% over two steps). ¹H NMR (CDCl₃, 400MHz) δ : 8.31 (d, $J = 7.6$ Hz, 1H, H-4'), 8.32-8.29 (m, 2H, H-5' and H-1'), 7.77 (t, $J = 7.6$ Hz, 1H, H-7'), 7.67 (t, $J = 7.6$ Hz, 1H, H-3'), 7.20 (t, $J = 7.6$ Hz, 1H, H-6'),

7.78 (br s, 2H, H-4 and H-5), 7.53 (br s, 1H, H-10''), 7.47 (t, $J = 7.6$ Hz, H-6'), 6.61 (d, $J = 8.0$ Hz, 1H, H-8'), 4.10 – 4.00 (m, 2H, CH₂), 3.99 – 3.92 (m, 4H), 3.63 (s, 3H, CH₃), 3.48 (q, $J = 6.8$ Hz, 1H), 3.22 (dd, $J = 17.4$ and 12.0 Hz, 1H, H-1'''), 3.06 (dd, $J = 17.4$ and 3.2 Hz, 1H, H-1'''), 1.61 – 1.48 (m, 2H), 1.38 – 1.18 (m, 19H), 0.89 – 0.82 (m, 12H, 4xCH₃) ppm. ESI-MS (m/z) (+): 315.1 [M]⁺, ESI-MS (m/z) (-): 421.2 [C₂₀H₃₇O₇S]⁻.

Cell culture. The biological assays were performed using a human ovarian carcinoma cell line (A2780), a human colorectal carcinoma cell line (HCT116), and human normal primary dermal fibroblasts, all purchased from ATCC (<http://www.atcc.org>). HCT116 cells and fibroblasts were cultured in Dulbecco's modified eagle medium (DMEM, ThermoFisher Scientific, Waltham, MA, USA), and A2780 cells were cultured in RPMI-1640 (ThermoFisher Scientific). All media were supplemented with 10 % (v/v) fetal bovine serum (ThermoFisher Scientific) and 1 % of antibiotic/antimycotic mixture (ThermoFisher Scientific). Experiments proceeded at 37 °C, 5 % (v/v) CO₂, 99 % (v/v) relative humidity unless stated otherwise.

Viability analysis using MTS assay. Dose-responses curves were determined by challenging the respective cell line to the individual compound and the cell viability was determined by the MTS assay. The compound solutions were prepared from a concentrated stock solution in DMSO. Cells were plated in 96-well plates in a cell density of 7500 cells/well. In a first screening, the media were replaced after 24 h with fresh media supplemented with 1 μM, 10 μM and 50 μM of each compound or 0.1 % (v/v) DMSO (vehicle control). After 48 h incubation, cell viability was evaluated using CellTiter 96 Aqueous One Solution Cell Proliferation Assay (Promega, Madison, WI, USA) as previously described [12, 47]. When at the maximum concentration tested for each compound (50 μM), the cell viability was

lower than 50 %, additional concentrations were tested to fine-tune the determination of the IC₅₀. The selectivity index was calculated as the ratio between the IC₅₀ of normal cells and the IC₅₀ of A2780 cells.

Internalization of compounds in A2780 through time. A2780 cells were seeded on 24-well plate at a density of 1×10^5 cells/well. After 24 h incubation, medium was removed and replaced by fresh medium supplemented with 0.1 % (v/v) DMSO (control), 125 μ M compound **1b** (10 x IC₅₀ for compound **1b** in A2780) or 11 μ M compound **1c** (10 x IC₅₀ for compound **1c** in A2780). After 1 h and 3 h incubation, cells were washed twice with PBS and fixed with 4 % (w/v) formaldehyde for 20 min. After washing three times with PBS, images of five random microscopic fields with circa 20 nuclei each were acquired using a Ti-U Eclipse inverted microscope (Nikon) and respective software, NIS Elements Basic software 3.1 (Nikon). For the same microscopic field images were acquired using phase contrast and a DAPI filter cube (Nikon; excitation filter with range between 340–380 nm and emission filter range at 435–485 nm). CTCF was calculated for each cell and fluorescence intensities corrected and normalized against the non-treated control sample.

Cell uptake of compounds in A2780 and HCT116. A2780 and HCT116 cells were seeded on 24-well plate at a density of 1×10^5 cells/well. After 24 h incubation, media were removed and replaced by fresh media supplemented with 0.1 % (v/v) DMSO (control), 125 μ M compound **1b** (10 x IC₅₀ for compound **1b** in A2780) or 11 μ M compound **1c** (10 x IC₅₀ for compound **1c** in A2780). After 3 h incubation either at 37 °C or 4 °C, cells were washed twice with PBS and fixed with 4 % (w/v) formaldehyde for 20 min. Image acquisition and analysis as described above.

Cytoskeleton stain. Following incubation of A2780 cells with each compound as described above for analysis of internalization, cells were fixed with 4 % (w/v)

formaldehyde for 20 min, washed three times with PBS and permeabilized with 0.1 % (v/v) Triton X-100 for 5 min. Cells were further incubated for 30 min with 1 % (w/v) Bovine Serum Albumin (BSA), stained with AlexaFluor 488 Phalloidin (ThermoFisher Scientific) according to the manufacturer's instructions and washed three times with PBS [48].

Nucleus staining with propidium iodide. A2780 cells were incubated with 11 μM compound **1c** as described above for the internalization analysis. Following 3 h incubation at 37 °C, cells were fixed for 20 min with 4 % (w/v) formaldehyde, washed 3 times with PBS, permeabilized for 5 min with 0.1 % (v/v) Triton X-100 and incubated for 30 min at 37 °C with 50 $\mu\text{g mL}^{-1}$ RNase H (Sigma). Cells were then washed three times with PBS, stained for 10 min with 2.5 $\mu\text{g mL}^{-1}$ Propidium iodide (ThermoFisher Scientific) and washed three times with PBS.

Viability analysis using Trypan Blue exclusion method. A2780 cells were seeded on a 24-well plate at a density of 37 500 cells/well. After 24 h, medium was replaced by fresh RPMI supplemented with 0.1 % DMSO or with three concentrations of compound **1b** and **1c** corresponding to: the IC_{50} , one concentration below (10x lower) and one above the IC_{50} (10x higher). After 48 h incubation, cells were detached from the well, centrifuged at 400 xg and pelleted cells resuspended in 0.2 % (w/v) Trypan Blue (ThermoFisher Scientific). The mixture was loaded on a haemocytometer (Hirschmann, Eberstadt, Germany) and viable cells counted in an Olympus CXX41 inverted microscope (Tokyo, Japan). Cell viability was calculated by normalizing the number of cells incubated with compound to that of cells incubated with DMSO [49].

Apoptosis analysis using Hoechst 33258 staining. A2780 cells were seeded in 24-well plate at a density of 37 500 cells/well. After 24 h, the medium was replaced

with fresh medium supplemented with 0.1 % (v/v) DMSO, the IC₅₀ of compound **1b** (12.5 µM) or the IC₅₀ of compound **1c** (1.1 µM). After 48 h incubation, cells were washed three times with phosphate buffer saline (PBS), fixed with 4 % (w/v) formaldehyde in PBS for 20 min, washed 3 times with PBS, incubated for 15 min with 7.5 µg mL⁻¹ Hoechst 33258 (ThermoFisher Scientific) and washed three times with PBS. Cell nuclei were visualized in a Ti-U Eclipse inverted microscope (Nikon, Tokyo, Japan) with a DAPI filter cube (Nikon; excitation filter with range between 340–380 nm and emission filter range at 435–485 nm) and images of five or more random microscopic fields containing 20 nuclei each (to ensure the analysis of at least 100 nuclei), were acquired using the microscopic software (NI-S Elements BR 3.10).

Apoptosis analysis using double staining. A2780 cells were seeded in a density of 100 000 cells/well in 6-well plate. After 24 h, the medium was substituted with fresh medium supplemented with 0.1 % (v/v) DMSO, 0.1 µM doxorubicin, 12.5 µM of compound **1b** (IC₅₀), 1.1 µM of compound **1c** (IC₅₀) or not supplemented (untreated). After 48 h incubation, cells were detached and double stained with Dead Cell Apoptosis kit with Annexin V - Alexa Fluor™ 488 & Propidium iodide (PI) (ThermoFisher Scientific) according to manufacturer's instructions. Fluorescence was quantified in an Attune focusing flow cytometer (ThermoFisher Scientific) and respective software, being considered unstained cells as live cells, cells stained only with Annexin V – Alexa Fluor™ 488 as cells in early apoptosis, cells stained only with PI as necrotic cells, and doubled stained cells as cells in late apoptosis.

Assessment of Mitochondria membrane potential. A2780 cells were seeded in 24-well plate at a density of 37500 cells/well. After 24 h, the medium was replaced with fresh medium supplemented with 0.1 % (v/v) DMSO, 0.1 µM Doxorubicin, 12.5 µM of compound **1b** (IC₅₀), or 1.1 µM of compound **1c** (IC₅₀). After 48 h, cells were

incubated with JC-1 dye (Abnova, Taipei, Taiwan) according to manufacturer's instructions and images of five random microscopic fields were immediately acquired using a Ti-U Eclipse inverted microscope (Nikon, Tokyo, Japan) using for the same field acquisition in contrast-phase, a green filter cube for JC-1 monomer acquisition (Nikon; excitation filter range of 465–495 nm and emission filter range at 515–555 nm) and a red filter cube for JC-1 aggregate acquisition (Nikon, excitation filter range of 510–560 nm and emission filter with wavelengths above 610 nm). The fluorescence of monomer and aggregate was quantified in an Attune focusing flow cytometer (ThermoFisher Scientific) and respective software. Values of JC-1 ratio were normalized to that of cells treated with DMSO.

Analysis of Autophagy. A2780 cells were seeded on a 6-well plate with a density of 100 000 cells/well. After 24 h incubation, medium was replaced by fresh medium supplemented with 0.1 % (v/v) DMSO, 0.4 μ M Rapamycin, 12.5 μ M of compound **1b** (IC_{50}), or 1.1 μ M of compound **1c** (IC_{50}). After 48 h, cells were detached from the well and treated with Autophagy detection kit (Abcam, Cambridge, UK) according to manufacturer's instructions. The fluorescence intensity of each sample was measured in an Attune focusing flow cytometer (ThermoFisher Scientific) and respective software.

Trypan Blue exclusion method for quantification of cells in the supernatant. A2780 cells were seeded on a 24-well plate at a density of 37 500 cells/well. After 24 h, medium was replaced by fresh RPMI supplemented with 0.1 % (v/v) DMSO, 1 μ M Doxorubicin (10 x IC_{50}), 125 μ M of compound **1b** (10 x IC_{50}), or 11 μ M compound **1c** (10 x IC_{50}). After 6 h incubation, the supernatant was collected, mixed with 0.2 % (w/v) Trypan blue and loaded on a haemocytometer (Hirschmann, Eberstadt, Germany). Viable (unstained) and dead (blue stained) cells were counted in an

Olympus CXX41 inverted microscope (Tokyo, Japan). Live and dead cells concentrations were normalized to the number of cells incubated with DMSO [42].

Western Blot for apoptotic index quantification. A2780 cells were seeded on T-flasks with an area of 25 cm² with a cell density of 750 000 cells/flask. After a period of 24 h incubation, medium was replaced by fresh RPMI supplemented with 0.1 % (v/v) DMSO, 0.1 μM Doxorubicin (IC₅₀), 12.5 μM of compound **1b** (IC₅₀), or 1.1 μM compound **1c** (IC₅₀). After 18 h or 48 h, cell monolayer was washed three times with PBS and scraped from the surface with a cell scraper in PBS. Cells were centrifuged at 500 *xg* and resuspended in lysis buffer (50 mM Tris-HCl, pH 8.0, 150 mM NaCl, 5 mM EDTA, 2 % (v/v) NP-40, 1 x phosphatase inhibitors (PhoStop, Roche), 1 x Protease inhibitors (complete Mini, Roche), 1 mM PMSF and 0.1 % (v/v) DTT). After 5 ultra-sound pulses, the suspension was centrifuged at 5 000 *xg* for 10 min and total protein extract (supernatant) was recovered and quantified with Pierce 660 nm Protein Assay Reagent (ThermoFisher Scientific). For SDS-PAGE, 10 μg protein was loaded on 10 % polyacrylamide gel and transferred to a 45 μm PVDF membrane (GE Healthcare). Membranes were blocked with 5 % (w/v) non-fat milk in Tris-buffered saline with 0.1 % (v/v) Tween-20 (TBST), incubated 1 h at RT with primary antibodies against BCL-2 (reference B3170, Sigma) and BAX (reference 32503, Abcam) and then with respective secondary antibodies conjugated with horseradish peroxidase (references 7074 and 7076, Cell Signalling Technology). The band intensity was acquired with WesternBright (Advansta) in a Hyperfilm ECL (GE Healthcare). The antibodies were stripped from the membrane with acidic stripping (0.1 M glycine, 20 mM magnesium acetate, 50 mM KCl, pH 2.2) and membrane was submitted to a new blockade with 5 % (w/v) non-fat milk in TBST, 1 h incubation with anti-β-actin (reference A5441, Sigma) and 1 h incubation with respective

secondary antibody (reference 7076, Cell Signalling technology). The protein band intensity was quantified using FIJI software [50]. The BAX and BCL-2 expression were quantified after normalization to β -actin values and then to values of the sample exposed to DMSO at the same time period of incubation. Apoptotic index was the ratio of BAX / BCL-2 expression.

Western Blot for E-cadherin expression quantification. The western blot for E-cadherin expression analysis followed the same procedure as described above for western blot for apoptotic index quantification with few alterations. Cells were only collected after 18 h incubation, 50 μ g of protein were applied for SDS-PAGE and the incubation with E-cadherin antibody (reference WH0000999M1, Sigma) was performed over night at 4 °C. The E-cadherin expression was quantified after normalization to β -actin and DMSO.

Caspase 8 activity. A2780 cells were seeded on 6-well plates in a density of 100 000 cells/well. After 24 h, medium was replaced by fresh medium supplemented with 0.1 % (v/v) DMSO, 0.1 μ M Doxorubicin (IC_{50}), 12.5 μ M of compound **1b** (IC_{50}), or 1.1 μ M compound **1c** (IC_{50}). After an incubation period of 18 h or 48 h, cells were detached using a cell scraper and pelleted using a centrifugation of 500 xg for 5 min. Samples were then treated as suggested by manufacturer of the Caspase-8 assay kit (Abcam). Data obtained for each sample was normalized to the value of the DMSO sample obtained for the respective period of incubation.

Relative Intracellular pH quantification. A2780 cells were seeded on 6-well plates at a density of 100 000 cells/well. After 24 h, medium was replaced by fresh RPMI supplemented with 0.1 % (v/v) DMSO, 0.1 μ M Doxorubicin (IC_{50}), 12.5 μ M of compound **1b** (IC_{50}), or 1.1 μ M compound **1c** (IC_{50}). After 3 h, 6 h, 18 h and 48 h cells were detached, pelleted with a 500 xg , 5 min centrifugation, washed once with

unsupplemented RPMI-1640 without phenol red through a centrifugation of 500 *xg*, 5 min, resuspended in 500 μ L 0.2 μ M BCECF-AM (Sigma) and incubated for 20 min at 37 °C. Cells were washed twice with unsupplemented RPMI-1640 without phenol red and fluorescence was acquired in a Attune focusing flow cytometer (ThermoFisher Scientific) and respective software. Values were normalized to the value of DMSO sample obtained in the respective period of incubation.

Quantification of Reactive Oxygen Species (ROS). A2780 cells were seeded in a 6-well plate at a density of 100.000 cells/well. After 24h, the medium was replaced with fresh medium supplemented with 0.1% (v/v) DMSO (vehicle control), 12.5 μ M compound **1b**, 1.1 μ M compound **1c** (IC₅₀ for either compound in A2780 cells), 25 μ M H₂O₂ (positive control for ROS induction) or not treated. After 48h incubation, cells were detached, pelleted by centrifugation at 500g for 5 min, washed twice with PBS, resuspended in 10 μ M 2,7-dichlorodihydrofluorescein diacetate (H₂DCF-DA) in PBS and incubated for 30 min. Data was acquired in an Attune acoustic focusing cytometer (ThermoFisher Scientific) by the measurement of the produced green fluorescent compound DCF formed by cleavage of H₂DCF-DA acetate groups by esterases and oxidation (excitation and emission at 492-495 nm and 517-527 nm, respectively). Fluorescence was normalized to that of untreated cells.

Statistical analysis. Data are expressed as mean \pm SEM of at least three independent experiments. Statistical significance was evaluated using Student t-test and a *p* value <0.05 considered statistically significant.

AUTHOR CONTRIBUTIONS

The manuscript was written through contributions of all authors. All authors have given approval to the final version of the manuscript. G. Malta and C. Roma-Rodrigues contributed equally to this work.

Acknowledgements

This work was supported by the Associate Laboratory for Green Chemistry-LAQV which is financed by national funds from FCT/MCTES (UIDB/50006/2020) and by the Applied Molecular Biosciences Unit- UCIBIO which is financed by national funds from FCT/MCTES (UID/Multi/04378/2020). The National NMR Facility and the SCXRD facility are supported by Fundação para a Ciência e Tecnologia (RECI/BBB-BQB/0230/2012 and RECI/BBB-BEP/0124/2012, respectively). We acknowledge the Laboratório de Análises REQUIMTE for the technical support for the mass spectrometry analyses.

REFERENCES

- [1] R. Anton and M. Haagberrurier, *Pharmacology* 20 (1980) 104-112.
- [2] E. M. Malik and C. E. Muller, *Med. Res. Rev.* 36 (2016) 705-748.
- [3] M. N. Preobrazhenskaya, A. E. Shchekotikhin, A. A. Shtil and H.-S. Huang, (2006) 26001.
- [4] H. Hussain, A. Al-Harrasi, A. Al-Rawahi, I. R. Green, R. Csuk, I. Ahmed, A. Shah, G. Abbas, N. U. Rehman and R. Ullah, *Expert Opin. Ther. Patents* 25 (2015) 1053-1064.
- [5] A. Rescifina, C. Zagni, M. G. Varrica, V. Pistara and A. Corsaro, *Eur. J. Med. Chem.* 74 (2014) 95-115.
- [6] J. V. McGowan, R. Chung, A. Maulik, I. Piotrowska, J. M. Walker and D. M. Yellon, *Cardiovasc. Drugs Ther.* 31 (2017) 63-75.
- [7] H. F. Li, M. D. H. Hassona, N. A. Lack, P. Axerio-Cilies, E. Leblanc, P. Tavassoli, N. Kanaan, K. Frewin, K. Singh, H. Adomat, K. J. Bohm, H. Prinz, E. T. Guns, P. S. Rennie and A. Cherkasov, *Mol. Cancer Ther.* 12 (2013) 2425-2435.
- [8] W. X. Hu and W. Zhou, *Bioorg. Med. Chem. Lett.* 14 (2004) 621-622.
- [9] H. Prinz, Y. Ishii, T. Hirano, T. Stoiber, J. A. C. Gomez, P. Schmidt, H. Dussmann, A. M. Burger, J. H. M. Prehn, E. G. Gunther, E. Unger and K. Umezawa, *J. Med. Chem.* 46 (2003) 3382-3394.
- [10] A. Zuse, H. Prinz, K. Muller, P. Schmidt, E. G. Gunther, F. Schweizer, J. H. M. Prehn and M. Los, *Eur. J. Pharmacol.* 575 (2007) 34-45.
- [11] J. F. Zhou, S. J. Tu and J. C. Feng, *J. Chem. Research* (2001) 414-415.
- [12] D. Peixoto, M. Figueiredo, G. Malta, C. Roma-Rodrigues, P. V. Baptista, A. R. Fernandes, S. Barroso, A. L. Carvalho, C. A. M. Afonso, L. M. Ferreira and P. S. Branco, *Eur. J. Org. Chem.*, DOI: 10.1002/ejoc.201701500 (2018) 545-549.
- [13] M. Blumel, R. D. Crocker, J. B. Harper, D. Enders and T. V. Nguyen, *Chem. Commun.* 52 (2016) 7958-7961.
- [14] A. Aupoix, B. Pegot and G. Vo-Thanh, *Tetrahedron* 66 (2010) 1352-1356.
- [15] N. Kumar and R. Jain, *J. Heterocycl. Chem.* 49 (2012) 370-374.

- [16] G. Descotes, J. P. Praly and A. Bouchu, *Carbohydr. Res.* 148 (1986) 137-142.
- [17] N. Jordao, H. Cruz, A. Branco, F. Pina and L. C. Branco, *ChemPlusChem* 82 (2017) 1211-1217.
- [18] R. J. Fakheri and F. M. Volpicelli, *J. Hosp. Med.* 14 (2019) 110-113.
- [19] H. L. Chen, H. F. Kao, J. Y. Wang and G. T. Wei, *J. Chin. Chem. Soc.* 61 (2014) 763-769.
- [20] A. A. Stepanenko and V. V. Dmitrenko, *Gene* 574 (2015) 193-203.
- [21] W. Strober, *Curr Protoc Immunol* (2001) Appendix 3, Appendix 3B.
- [22] S. J. Korsmeyer, J. R. Shutter, D. J. Veis, D. E. Merry and Z. N. Oltvai, *Semin Cancer Biol* 4 (1993) 327-332.
- [23] M. S. D'Arcy, *Cell Biol. Int.* 43 (2019) 582-592.
- [24] E. A. Prokhorova, A. V. Zamaraev, G. S. Kopeina, B. Zhivotovsky and I. N. Lavrik, *Cell. Mol. Life Sci.* 72 (2015) 4593-4612.
- [25] N. N. Danial and S. J. Korsmeyer, *Cell* 116 (2004) 205-219.
- [26] C. M. Pfeffer and A. T. K. Singh, *Int. J. Mol. Sci.* 19 (2018).
- [27] S. Elmore, *Toxicol. Pathol.* 35 (2007) 495-516.
- [28] J. D. Ly, D. R. Grubb and A. Lawen, *Apoptosis* 8 (2003) 115-128.
- [29] A. Perelman, C. Wachtel, M. Cohen, S. Haupt, H. Shapiro and A. Tzur, *Cell Death Dis.* 3 (2012).
- [30] K. A. Koeplinger, A. M. Mildner, J. W. Leone, J. S. Wheeler, R. L. Heinrikson and A. G. Tomasselli, *Protein Expr. Purif.* 18 (2000) 378-387.
- [31] C. Dive, J. V. Watson and P. Workman, *Cytometry* 11 (1990) 244-252.
- [32] M. O. Bevenssee, C. J. Schwiening and W. F. Boron, *J. Neurosci. Methods* 58 (1995) 61-75.
- [33] A. L. Grenier, K. Abu-Ihweij, G. Zhang, S. M. Ruppert, R. Boohaker, E. R. Slepokov, K. Pridemore, J. J. Ren, L. Fliiegel and A. R. Khaled, *Am. J. Physiol.-Cell Physiol.* 295 (2008) C883-C896.
- [34] A. Ishaque and M. Al-Rubeai, *J. Immunol. Methods* 221 (1998) 43-57.
- [35] S. H. M. Wong, C. M. Fang, L. H. Chuah, C. O. Leong and S. C. Ngai, *Crit. Rev. Oncol./Hematol.* 121 (2018) 11-22.
- [36] S. Galaz, J. Espada, J. C. Stockert, M. Pacheco, F. Sanz-Rodriguez, R. Arranz, S. Rello, M. Canete, A. Villanueva, M. Esteller and A. Juarranz, *J. Cell. Physiol.* 205 (2005) 86-96.
- [37] M. Lu, S. Marsters, X. F. Ye, E. Luis, L. Gonzalez and A. Ashkenazi, *Mol. Cell* 54 (2014) 987-998.
- [38] O. Tacar, P. Sriamornsak and C. R. Dass, *J. Pharm. Pharmacol.* 65 (2013) 157-170.
- [39] P. Ozkan and R. Mutharasan, *Biochim. Biophys. Acta-Gen. Subj.* 1572 (2002) 143-148.
- [40] P. Weerasinghe and L. M. Buja, *Exp. Mol. Pathol.* 93 (2012) 302-308.
- [41] B. F. Trump, I. K. Berezsky, S. H. Chang and P. C. Phelps, *Toxicol. Pathol.* 25 (1997) 82-88.
- [42] K. A. Elliget, P. C. Phelps and B. F. Trump, *Cell Biol. Toxicol.* 7 (1991) 263-280.
- [43] M. L. Chen, L. Yi, X. Jin, Q. Xie, T. Zhang, X. Zhou, H. Chang, Y. J. Fu, J. D. Zhu, Q. Y. Zhang and M. T. Mi, *J. Nutr. Biochem.* 24 (2013) 1823-1829.
- [44] Y. Q. Sun, J. H. Lu, D. X. Yan, L. P. Shen, H. Y. Hu and D. W. Chen, *Environ. Toxicol. Pharmacol.* 53 (2017) 46-56.
- [45] S. J. Korsmeyer, X. M. Yin, Z. N. Oltvai, D. J. Veisnovack and G. P. Linette, *Biochim. Biophys. Acta-Mol. Basis Dis.* 1271 (1995) 63-66.

- [46] F. Yang, S. S. Teves, C. J. Kemp and S. Henikoff, *Biochim. Biophys. Acta-Rev. Cancer* 1845 (2014) 84-89.
- [47] N. Svahn, A. J. Moro, C. Roma-Rodrigues, R. Puttreddy, K. Rissanen, P. V. Baptista, A. R. Fernandes, J. C. Lima and L. Rodriguez, *Chem.-Eur. J.* 24 (2018) 14654-14667.
- [48] C. Roma-Rodrigues, C. Alves-Barroco, L. R. Raposo, M. N. Costa, E. Fortunato, P. V. Baptista, A. R. Fernandes and I. Santos-Sanches, *Microbes Infect.* 18 (2016) 290-293.
- [49] A. Maron, K. Czerwinska, B. Machura, L. Raposo, C. Roma-Rodrigues, A. R. Fernandes, J. G. Matecki, A. Szlapa-Kula, S. Kula and S. Krompiec, *Dalton Trans.* 47 (2018) 6444-6463.
- [50] J. Schindelin, I. Arganda-Carreras, E. Frise, V. Kaynig, M. Longair, T. Pietzsch, S. Preibisch, C. Rueden, S. Saalfeld, B. Schmid, J. Y. Tinevez, D. J. White, V. Hartenstein, K. Eliceiri, P. Tomancak and A. Cardona, *Nat. Methods* 9 (2012) 676-682.



- Synthesis of structural diverse arylidene anthrones.
- Antiproliferative effect related to the imidazolium pattern of the heterocyclic.
- The mechanism of cytotoxicity is different from that of doxorubicin.
- Compounds showing antiproliferative selectivity towards ovarian cancer cells.